Spectrochimica Acta Part A: Molecular and Biomolecular Spectroscopy 325 (2025) 125144

Contents lists available at ScienceDirect

Spectrochimica Acta Part A:
Molecular and Biomolecular Spectroscopy

journal homepage: www.journals.elsevier.com/spectrochimica-acta-part-a-molecular-and-biomolecular-spectroscopy

Effect of gamma radiation on freeze-dried red pitaya (*Hylocereus costaricensis*) skin powder: An EPR study to assess the original dose

Luz M. Rondán-Flores [a], T.K. Gundu Rao [b], Anna L.C.H. Villavicencio [a], Nilo F. Cano [c,*]

[a] *Instituto de Pesquisas Energéticas e Nucleares, IPEN/CNEN-SP, São Paulo, SP, Brazil*
[b] *Universidad Nacional de San Agustín de Arequipa, UNSA, Arequipa, Peru*
[c] *Universidade Federal de São Paulo, UNIFESP, Santos, SP, Brazil*

HIGHLIGHTS

- Red pitaya shell powder was characterized by SEM, XRD and EPR spectroscopy.
- No significant change in the state of crystalline cellulose and glucose in the skin powder, between 500 Gy and 30 kGy.
- Gamma irradiation induced two free radical centers.
- Pitaya samples can be used in diagnostic irradiation applications.

GRAPHICAL ABSTRACT

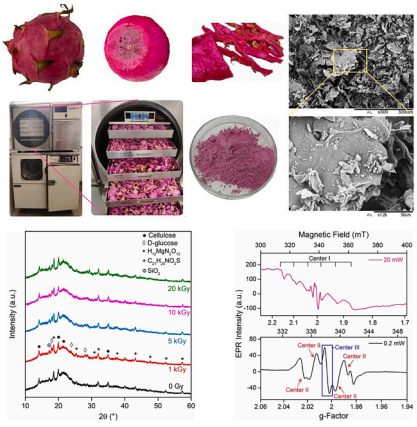

ARTICLE INFO

Keywords:
Dragon Fruit
EPR
Free radicals
Gamma radiation
XRD

ABSTRACT

The integral use of some fruits is an alternative for sustainable production from an environmental, social, and economic point of view, so activities that promote the sustainability of the food production chain, such as fruits waste irradiation, are being carried out. For control and safety purposes with irradiated products, it is necessary to use precise and adequate techniques that allow the marking and unequivocal identification of these products. Among these techniques, electron paramagnetic resonance (EPR) spectroscopy has stood out for its high sensitivity in detecting paramagnetic species generated during irradiation. The pitaya fruit has as its processing residue its skin, which represents 33 % of its total weight. In addition, studies carried out with pitaya reveal the presence of bioactive compounds, including phenolic compounds, that contribute to its antioxidant capacity. With this perspective, in the present work, we investigated the paramagnetic centers induced by gamma irradiation in powdered red pitaya skin products by means of the EPR technique, with the purpose of using them as indicators and/or dosimetric material for the determination of the absorbed dose in irradiated pitaya skin products. EPR experiments indicate the presence of at least three paramagnetic species. One of the centers (center I) exhibits six hyperfine lines with g = 2.0050 and is attributed to the Mn^{2+} ion. Center II has

* Corresponding author.
E-mail addresses: lrondanf@alumni.usp.br (L.M. Rondán-Flores), nilocano@if.usp.br, nilo.cano@unifesp.br (N.F. Cano).

https://doi.org/10.1016/j.saa.2024.125144
Received 19 July 2024; Accepted 12 September 2024
Available online 14 September 2024

contributions from at least two radicals, and the dominant radical displays hyperfine interaction with one α-type and two nearly equivalent β-type protons with g = 2.0042. Center III has g = 2.0029 and results from the cellulosic part of the pitaya fruit. The intensity of centers II and III increases linearly with increasing gamma irradiation doses in the dose range from 500 Gy to 30 kGy. In addition, the fading results with storage time at room temperature of centers II and III show a 20 % decay in the first 21 days and then stabilize. Also, complementary studies of the morphology and degree of crystallinity of the pitaya skin powder were carried out by scanning electron microscopy (SEM) and X-ray diffraction (XRD), respectively.

1. Introduction

Nowadays, socioeconomic development and environmental sustainability are fundamental aspects of any society, and it is urgent to combine increased food production with the fulfillment of the Sustainable Development Goals (SDGs) [1], through the use of technologies that reduce losses and waste, and that allow reaching new markets. Data indicate that 1.3 billion tons are lost, which is equivalent to one-third of the food produced, even before reaching the consumer, due to failures in the production, conservation, storage, and transport chain [2].

Agro-industrial wastes include a wide variety of materials with the potential to generate subproducts. Among them, we have stalks, seeds, molasses, barks, and skins [3]. In addition to the great diversity of these agro-industrial wastes, there is growing concern about the rising amount of agro-industrial waste and the methods used for its disposal, which can negatively impact the environment. Therefore, several studies are being developed to transform these wastes into products with high-added value to be reused, either for consumption or for a specific application [4].

The process of reutilization of agro-industrial wastes allows the development of by-products with high aggregate value of the material that would be discarded in principle [5]. In addition, in the reutilization process, it is necessary to treat the waste to reduce the microbial charge to ensure its safety and reduce its perishability without losing its nutritional properties. In this regard, irradiation with ionizing radiation stands out as a well-established technique for food preservation. Among the main advantages of ionizing radiation are: reduction of the general microbial charge, disinfestation of insects, eggs, and larvae, inhibition of sprouting, delayed ripening of fresh fruits and vegetables, and increased shelf life of various foods. Depending on the dose of ionizing radiation the organoleptic and nutritional characteristics of the product can be preserved [6,7]. Therefore, it is necessary to control the amount of radiation dose to which a given product or agro-industrial subproduct is subjected.

Distinguishing an irradiated food from non-irradiated foods and measuring the radiation dose to which it was exposed are important data to guarantee the quality and safety of a given food product or by-product and, as a consequence, increase the acceptability of irradiated foods. For this purpose, it is necessary to have precise techniques that allow identifying irradiated foods and measuring the radiation dose used.

Some techniques have been used to detect irradiated foods satisfactorily for control purposes and to determine the amount of dose to which a food was subjected [8,9]. Among the spectroscopic techniques that stand out is electronic paramagnetic resonance (EPR) for its high sensitivity for the detection of free radicals generated in irradiated foods [10].

EPR is a technique that detects ions or molecules with unpaired electrons, such as free radicals [11]. When foods are treated with ionizing radiation, free radicals can be formed, so the EPR technique can be applied to monitor and quantify the radiation dose to which a food was subjected [12]. The concentration of free radicals formed during irradiation is directly proportional to the intensity of the EPR signal [11].

The exploration of the micromorphological characteristics of food products by scanning electron microscopy (SEM) is one of the best high-resolution technologies to understand the morphological characteristics of the surfaces of freeze-dried and crushed food product grains. In addition, it is possible to study the size distribution of particles that are useful for use in conventional and healthy products, such as ingredients in food formulas [13]. On the other hand, X-ray diffraction (XRD) is another important technique that has been used to characterize and evaluate the presence of crystal structures in dehydrated foods and to detect any changes in the crystallinity of the pattern of these structures due to different processing techniques [14,15].

Pitaya fruit (dragon fruit) has nutritional and functional characteristics that make its cultivation promising [16]. Both the pulp and skin of the fruit are a source of fiber with attractive digestive attributes [17–19]. Its physical and chemical characteristics may vary from species to species due to the high genetic diversity of this fruit [20–22]. In addition, research on pitaya reveals the presence of bioactive compounds, including phenolic compounds such as flavonoids, which contribute to the antioxidant capacity of this fruit [23–25]. The beneficial effects of these compounds are related to the prevention of degenerative diseases such as colon cancer, and diabetes mellitus, and the reduction of bacterial infections and cardiovascular diseases [26,27]. Particularly, red pitaya possesses the betalain group of phenolic compounds, which are divided into betaxanthins (yellow color) and betacyanins (violet color) [28].

European Committee of Normalization standards exist for the use of the EPR technique for the detection of radiation in specific food products and by-products containing stone, cellulose and crystalline sugar [29–31]. However, recent studies show that depending on the way a product is prepared, such as the method of dehydration of a fruit, the EPR spectrum may have different results [32,33].

There are no studies on the identification of paramagnetic centers and their behavior with gamma radiation dose in dehydrated pitaya skin samples. Therefore, the present work reports the identification and behavior of paramagnetic centers in pitaya skin subjected to different doses of gamma radiation in order to make feasible the use of EPR as a technique to control and determine the radiation dose to which the pitaya was subjected. In addition, complementary studies of the structure and morphology were carried out using X-ray diffraction (XRD) and scanning electron microscopy (SEM) techniques, respectively, in order to identify the presence of crystalline phases and the uniform distribution of the pitaya skin powder.

2. Material and methods

2.1. Sample and sample's preparation

Fig. 1(a) shows red pitaya fruits of variety *Hylocereus costaricensis*, produced in the interior of the State of São Paulo and purchased at the CEAGESP (Companhia de Entrepostos e Armazéns Gerais de São Paulo) supply center in the city of São Paulo, Brazil. The pitaya fruits were transported to the Laboratory for Analysis and Detection of Irradiated Foods (LADAI) of the Radiation Technology Center (CTR) of the Nuclear and Energy Research Institute (IPEN/CNEN-SP).

The red pitaya fruits were selected in relation to their physical appearance, which was free of external lesions on their skin. All fruits were first washed to remove surface impurities and rinsed under running water, then submerged for 10 min in a sodium hypochlorite solution at 100 µl/L and further rinsing with running water.

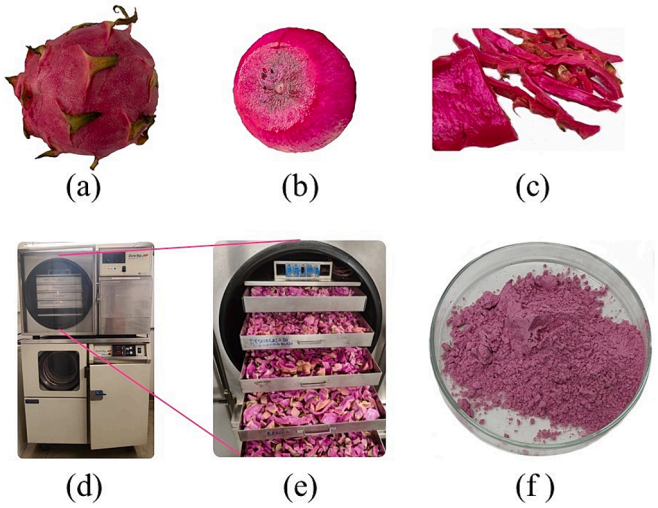

Fig. 1. (a) Red pitaya fruit, (b) pulp of pitaya fruit, (c) red pitaya skin for dehydration process, (d) freeze dryer used to dehydrate pitaya skin, (e) Freeze-dried pitaya skin, and (f) dehydrated pitaya skin particles with diameters less than 200 μm.

Once hygienized, the red pitaya fruits were pulped (Fig. 1(b)), and the skins of the fruits (Fig. 1(c)) were packed in polyethylene plastic bags of 200 g each and stored in a cold room at a freeze temperature of −80 °C to preserve their physicochemical properties. The dehydration process of the skin was carried out by the lyophilization method (Fig. 1(d and e)).

Pitaya skin dehydration experiments were conducted in a pilot-scale freeze dryer (Freeze dryer Dura-Top/Dura Stop MP, Dura Dry MP, FTS Systems™, Stone Ridge). Pitaya skins were frozen at −35 °C and held for 2 h to achieve ice crystallization, then dried at a storage temperature of −40 °C, and the final product temperature was set at 30 °C. Completely dried pitaya skin samples were ground for 4 h at 250 rpm with a horizontal cylindrical mill, brand Quimis, model Q2932, of 18 cm radius and 26 cm height containing 2 cm-diameter alumina balls, and then sieved using a standard stainless-steel mesh to obtain pitaya particles with a size less than 200 μm (Fig. 1(f)). Subsequently, the powdered pitaya skin samples were weighed, stored in hermetically sealed aluminum foil bags using a vacuum sealer, and stored at room temperature.

2.2. Instrumentation

2.2.1. Scanning electron microscope (SEM)

Morphological analysis of the fine grains of dried red pitaya was performed with a scanning electron microscope (SEM), Hitachi, model TM 3000, of the Center of Science and Technology of Materials (Centro de Ciência e Tecnologia de Materiais - CCTM) of IPEN. Prior to SEM analysis, all samples were coated with a thin layer of gold particles by sputtering in high vacuum in order to make them electrically conductive. SEM images were recorded at 300 and 1200 magnification.

2.2.2. X-ray diffraction (XRD)

XRD measurements to determine the formation of crystalline and/or amorphous phases in freeze-dried pitaya skin with and without gamma irradiation dose were recorded using an X-ray diffractometer Rigaku, model Miniflex 300, with CuKα radiation, with a voltage of 40 kV and a current of 25 mA. The powdered sample was lightly pressed on a glass sample holder using a glass slide and then scanned for a region of diffraction angles (2θ) between 10° and 60°, with an increasing step of 0.02°.

2.2.3. Electron paramagnetic resonance (EPR)

EPR spectra were recorded at room temperature with a Bruker spectrometer using the X-band microwave frequency. The recording parameters of the EPR spectra were: a center field of 337 mT, a modulation amplitude of 0.2 mT, a modulation frequency of 100 kHz and microwave powers between 0.002 and 80 mW. Samples of pitaya powder with a mass of 150.0 ± 0.1 mg, irradiated with gamma rays at room temperature, were placed in quartz tubes with an internal diameter of 4 mm, which in turn were placed inside the EPR cavity. To discriminate and identify the paramagnetic centers responsible for the EPR signals, the EPR spectra of an irradiated sample subjected to different annealing temperatures in the range 50–140 °C with 10 °C steps were recorded. The EPR intensity was measured by the peak-to-peak amplitude.

2.3. Irradiation

Irradiations of powdered pitaya samples for doses in the region of 500 Gy to 30 kGy were carried out at IPEN's Radiation Technology Center (CTR – *Centro de Tecnologia das Radiações*) using a gamma-cell Co-60 source with a dose rate of 0.64 kGy/h. All gamma irradiations were performed at room temperature.

3. Results and discussion

3.1. Scanning electron microscopy (SEM)

The SEM images in Fig. 2 show the microstructure of the red pitaya skin at a magnification scale of x300 and x1200. This morphological study reveals the presence of slight wrinkles with irregular geometry on the surface of red pitaya particles. Similar results were found by Chia and Chong [34] on crushed pitaya skin samples. Meanwhile, in a recent study, Taharuddin et al. [35] stated that the presence of irregular wrinkles on the surface of pitaya is due to the drying process as well as the physical process of crushing. During the grinding process carried out with alumina spheres in this work, they produce friction and shearing randomly on the lyophilized pitaya skin, which causes a rough and irregular surface.

3.2. X-ray diffraction (XRD)

X-ray diffraction (XRD) is a technique used to analyze the crystalline and/or amorphous state of organic and inorganic materials in powder form. A crystalline material presents sharp peaks in the XRD spectrum. On the other hand, materials with amorphous structures present a pattern in the form of a broad band. This is because the constituents (whether atoms or molecules) of the material do not form any regular repeating pattern in its structure.

The XRD analysis is of fundamental importance to demonstrate the structural state of the red pitaya powders in relation to the radiation doses to which they were subjected. In addition, it allows to verify the presence of crystalline phases formed during the drying process of red pitaya skins by freeze-drying.

Fig. 3 shows the XRD spectra profile of the red pitaya powders without irradiation and irradiated with gamma radiation with doses of 1, 5, 10, and 20 kGy. For each dose, XRD measurements were taken in triplicate. All the diffractograms of the irradiated samples are similar to the spectrum of the non-irradiated sample. This result indicates that irradiation does not produce significant changes in the crystalline and/or amorphous structure of the freeze-dried red pitaya skin.

According to the XRD profile in Fig. 3, the red pitaya sample shows amorphous and crystalline structures. The peaks defined at 14°, 20°, 22° and 35° may be associated with the presence of mainly cellulose [35–37], which is to be expected since the skins is constituted of

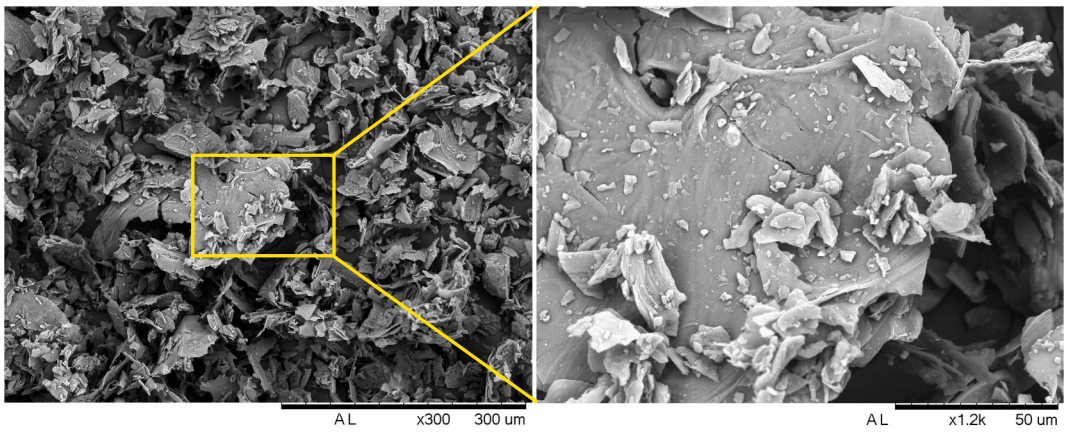

Fig. 2. SEM of the surface structure of powdered pitaya skin at 300x (left) and 1200x (right) magnification.

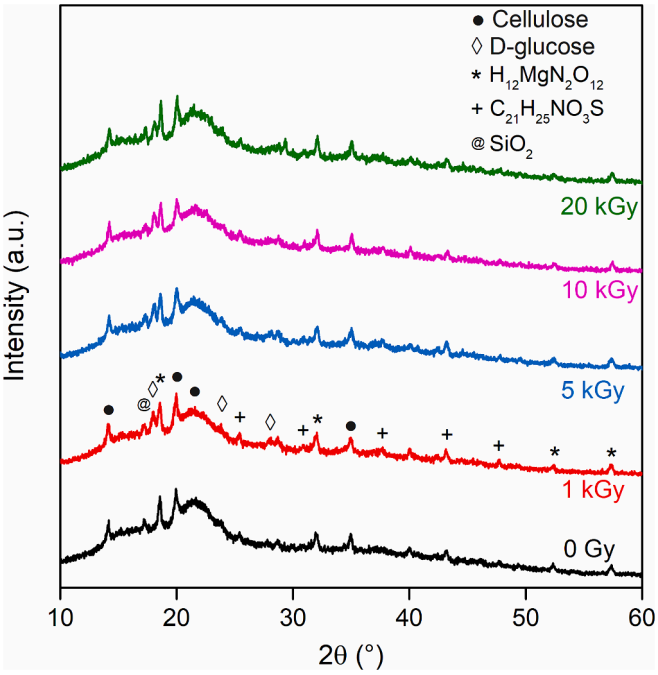

Fig. 3. X-ray diffraction spectrum of dehydrated red pitaya in powder form and irradiated with gamma radiation doses of 1, 5, 10 and 20 kGy.

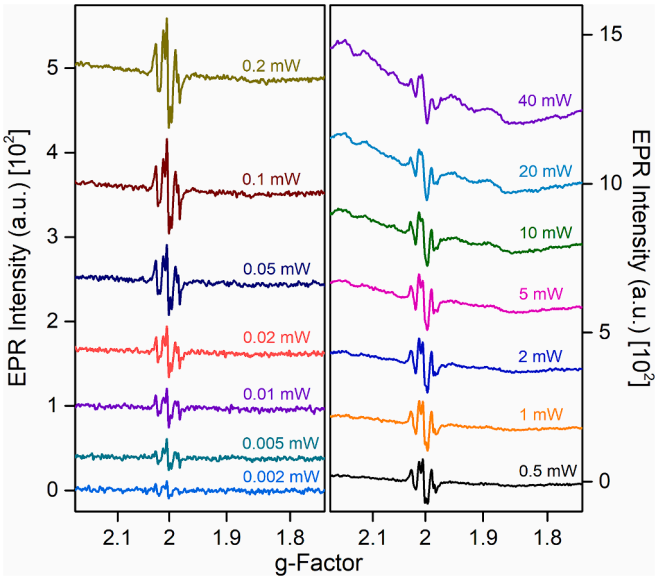

Fig. 4. EPR spectra obtained for different microwave powers from 0.002 to 40 mW of the red pitaya sample irradiated with a gamma radiation dose of 10 kGy.

cellulose, and the diffraction peaks at 2θ = 19°, 24° and 28° are due to the presence of sugar in the form of D-glucose [38,39]. Other low intensity diffraction peaks were identified due to the presence of $H_{12}MgN_2O_{12}$, $C_{21}H_{25}NO_3S$, and SiO_2 molecules [40]. The predominance of crystalline material in the samples can be explained by the fact that, during the drying process, the product reached the necessary conditions to produce a large number of organic crystals. A similar situation was observed by Otálora et al. [40], Harnkarnsujarit and Charoenrein [39], Pereira et al. [41] when they analyzed XRD plots for freeze-dried yellow pitaya, manga, and pineapple skin powders, respectively, revealing amorphous characteristics and presence of crystalline peaks.

3.3. Electron paramagnetic resonance (EPR)

Before performing the study to identify the free radicals (paramagnetic centers) generated during irradiation and their dependence on dose, as well as to investigate the fading of each EPR signal with storage time, the effect of microwave power on the EPR spectrum was investigated. Microwave power is one of the main parameters affecting EPR measurements, so it is necessary to establish an adequate power to observe all signals in the EPR spectrum without entering the saturation region.

Fig. 4 shows the room temperature EPR spectra of red pitaya irradiated with a gamma radiation dose of 10 kG for different microwave powers between 0.002 mW and 40 mW. The EPR spectrum for a power of 0.2 mW shows well-defined EPR lines (in the region of $g = 2.0$) with higher EPR intensity. For microwave powers above 10 mW it is possible to observe broad signals superimposed on the signals in the region of $g = 2.0$.

Fig. 5 shows the behavior of the peak-to-peak EPR signal intensity as a function of the square root of the microwave power for red pitaya subjected to a gamma radiation dose of 10 kGy. The EPR intensity of both EPR signals in the region of $g = 2.0$, referred to here as centers II and III, increase with the square root of the microwave power up to at least 1 mW and 1.8 mW, respectively, without saturation. For powers above these values, the EPR intensity saturates and then decays as the microwave power increases. Similar results were observed by Jesus et al. [42], Chiappinelli et al. [43], Paksu et al. [44], and Maghraby et al. [45] on freeze-dried fruits. In this work, EPR measurements were performed with a microwave power of 0.02 mW because it is in the linear region and with this value, we found a good increase in EPR intensity,

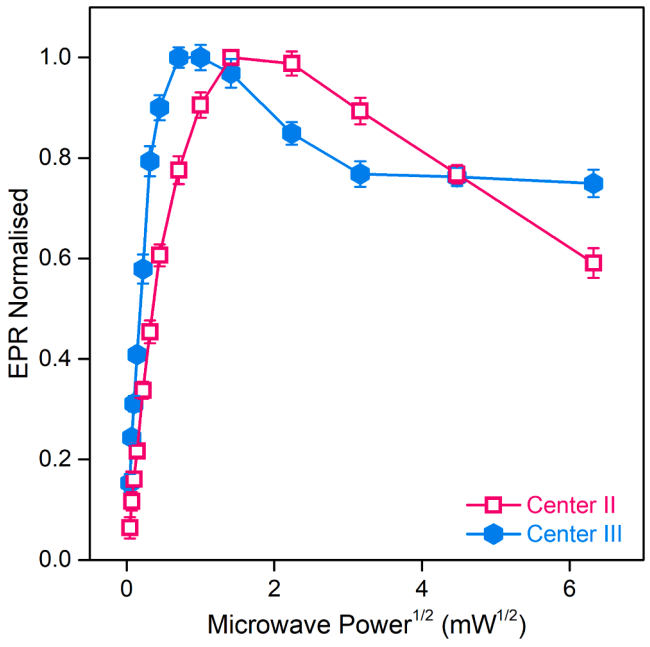

Fig. 5. Variation of EPR intensity vs. square root of microwave power.

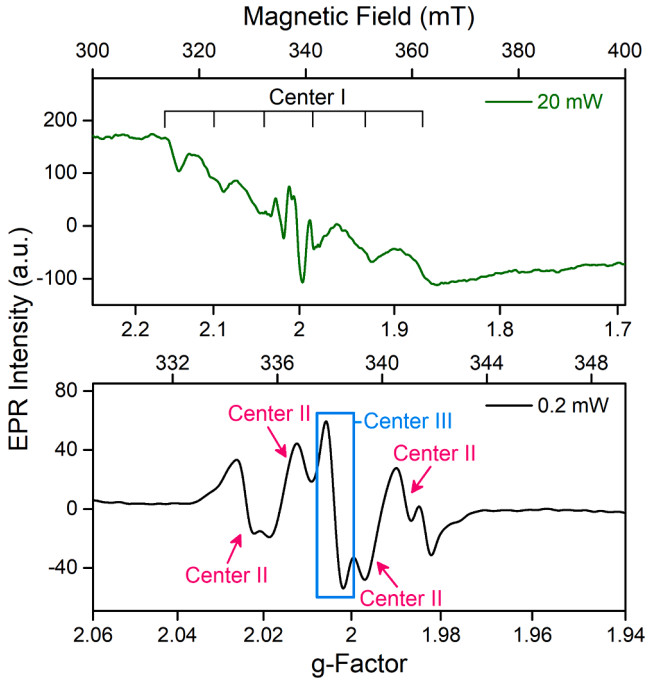

Fig. 6. Room temperature EPR spectra of gamma irradiated (dose: 10 kGy) red pitaya powder. The lines from the center I are shown by the stick lines. These lines are from the Mn^{2+} ion. Lines of center II are attributed to the "sugar-like" spectrum observed in sugar samples and are indicated in the spectrum of the red pitaya sample. Center III is due to the radical derived from the cellulose part of the pitaya fruit.

increasing the signal-to-noise ratio without entering the saturation region for EPR signals in the region of $g = 2.0$.

The room temperature EPR spectra of gamma irradiated red pitaya powder are shown in Fig. 6. Observation of the spectra at different MW powers along with thermal anneal experiments show that the observed spectrum has contributions from at least three paramagnetic species. The three defect centers are labelled in Fig. 6.

Center I is composed of six EPR lines and it is observed that not all six lines are clearly seen in Fig. 6 (top). This is due to the overlap of the fourth line with EPR lines around $g = 2.0$. A similar result was obtained by Saenjum et al. [46] on the EPR spectra of red and white pitaya. Some of them are broadened and the intensity of these lines is not high. The g-value of this species is estimated to be about 2.0050 and the separation between the successive individual lines is 92 Gauss.

Based on thermal annealing experiments, it is inferred that the lines of center I belong to a single paramagnetic species. The observed g-value is close to the free-electron value (2.0023) and the center is observable at room temperature. The six-line spectrum is more clearly seen in the red pitaya sample for a microwave power of 20 mW. The spectrum recorded after high-temperature thermal anneal is shown in Fig. 7.

On the basis of the stability of the center I at high temperatures, it is inferred that the signal possibly arises from a transition metal ion. Further, it is assumed that the ion belongs to the iron group. Among the iron group ions, Fe^{3+} and Mn^{2+} ions have a g-value close to 2.0 and it is possible to observe the EPR spectrum at room temperature. Further, six fine structure lines are expected for the Mn^{2+} ion and the ion displays hyperfine lines (I=5/2) [47]. The six hyperfine lines are due to the interaction between the electron spin (S=5/2) and the nuclear spin (I=5/2) of the Mn^{2+} ion ($3d^5$) and are due to the transitions $\Delta M_S = \pm 1$ and $\Delta M_I = 0$. In a powder sample, only the central fine structure line is observed as the other lines are broadened due to the anisotropy of the fine structure lines. Based on these observations, the lines of center I are assigned to the Mn^{2+} ion. Mn^{2+} is naturally present in the pitaya fruit and possibly accumulated from the soil in the pitaya plant where it participates in the process of photosynthesis [48].

Several lines are observed near the $g = 2.0$ region (Fig. 6). They have much higher intensities as compared to the Mn^{2+} lines. Among these lines, lines labeled as center II show approximately the same thermal annealing behavior. The thermal annealing behavior is shown in Fig. 8. These features indicate that the lines belong to a single paramagnetic species.

Irradiated fruits have been studied using the EPR technique [49,50]. In addition to several radical species, a common spectrum in different fruits, is usually observed and is termed a "sugar-like" spectrum [51]. The spectrum observed in dry fruits is very similar to the spectra of D-glucose, D-fructose, and sucrose. Fruits contain sugars of different kinds like fructose, glucose, etc. Pitaya, being a fruit, has sugar as one of its

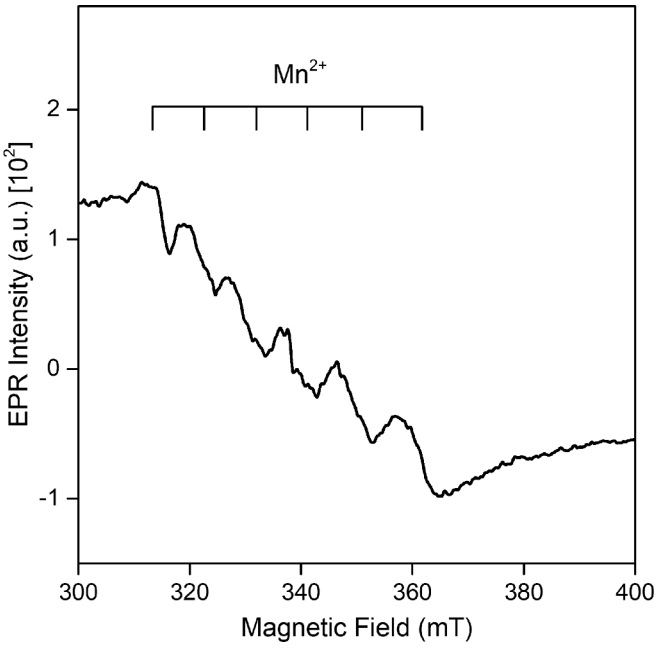

Fig. 7. Room temperature EPR spectrum of red pitaya powder after thermal annealing at 250 °C.

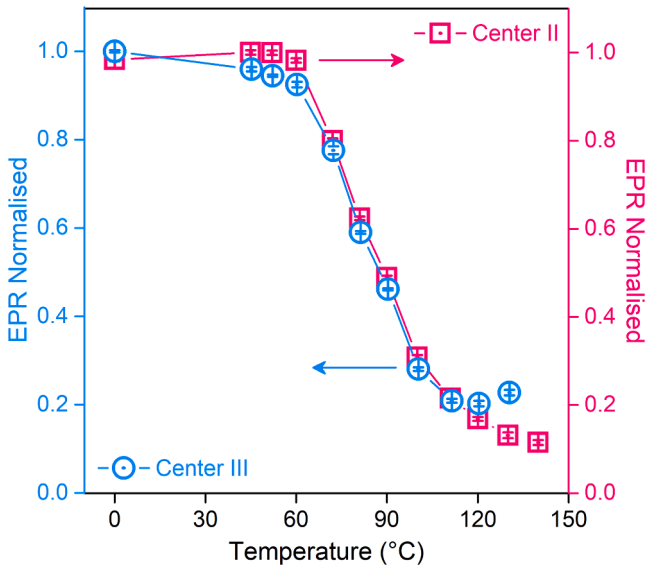

Fig. 8. Thermal annealing behavior of different lines of center II and center III in red pitaya powder.

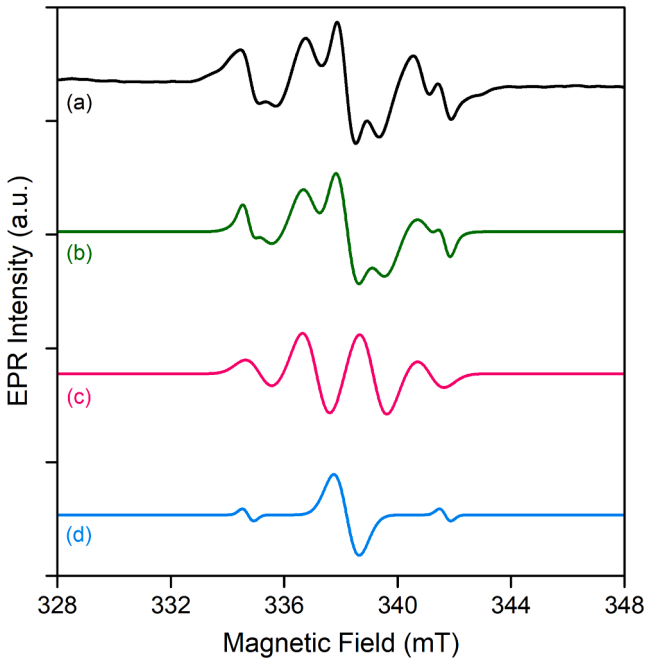

Fig. 9. Simulated and experimental EPR spectra in red pitaya sample. The experimental spectrum is labeled as (a). The simulated spectrum of center II and center III are labeled as (c) and (d) respectively. The combined simulated spectrum of centers II and III is labeled as (b).

constituents. In the early work on irradiated sucrose, numerous studies were carried out to understand and identify the radicals formed in the system. Shields and Hamrich [52] and Lomaglio [53] inferred that the observed spectrum can be understood in terms of a doublet of 1:2:1 triplet. The spectrum arises from one α-type and two nearly equivalent β-type proton couplings. Later, Gräslund and Löfroth [54] indicated the absence of symmetry in the EPR spectrum and interpreted the spectrum as due to the overlap of the EPR spectra from two radical species. Each one of these species was characterized by a hyperfine interaction of the unpaired electron with one α-type and one β-type proton interaction. Subsequently, Sagstuen et al. [55] re-examined the EPR spectrum of irradiated sucrose using EPR measurements at X-band and Q-band frequencies complemented by electron nuclear double resonance (ENDOR) spectroscopy. Based on this detailed study, particularly with the help of ENDOR, they inferred the existence of at least two radical species. A definitive assignment was made for one of the species and this species is identified as a radical of the type $RCO\dot{C}HCH_2$. The second species is possibly of this type characterized by one α-type and two β-type proton hyperfine interactions.

By carrying out a statistical analysis of the irradiated sucrose powder along with EPR, ENDOR, and ENDOR-induced EPR (EI-EPR) results on sucrose single crystals, Vanhaelewyn et al. [56] concluded that three similar radicals (S1, S2, and S3) are the major contributors to the observed spectra. S1 radical is most probably the $RCO\dot{C}HCH_2$ radical identified by Sagstuen et al. [55]. S2 and S3 are likely to be the second species assigned in the study of Sagstuen et al. [55]. They also mention that the statistical method indicates the presence of at least three more minor components (radicals).

Center II observed in the present study (Fig. 6) on pitaya fruit is characterized by a *g*-value of 2.0035. The spectrum appears to be composed of two triplets with a 1:2:1 intensity ratio and with $A_\alpha = 28.4$ G and $A_\beta = 25.7$ G. These are approximate values as there is an overlap of lines from other low-intensity radicals. Based on the observed features of the radicals in sucrose studied previously, in particular, the study by Sagstuen et al. [55], the center II spectrum is considered as a "sugar-like" spectrum with a dominant contribution coming from a radical of the type $RCO\dot{C}HCH_2$. An EPR spectral simulation has been carried out and the parameters used for center II simulation are: $g = 2.0035$, $A_\alpha = 28.4$ G, and $A_\beta = 25.7$ G. This simulated spectrum is shown in Fig. 9. An additional isotropic single line with a *g*-value equal to 2.0029 along with the satellite lines is superposed to obtain a good fit with the experimentally observed spectrum. This additional line is center III observed in the present study.

The stability of center II was determined using the pulse-thermal annealing method. The sample was heated to a specific temperature and held at that temperature for three minutes before being cooled to room temperature for EPR measurements. Fig. 8 shows the thermal annealing behavior of center II. Center II becomes unstable around 60 °C and undergoes decay in the temperature range of 60 °C to 140 °C (Fig. 8).

Gamma-irradiated fruits, in general, display a triplet spectrum arising from a radical induced in the cellulosic part of the fruit [57]. It has been mentioned that it can be observed in all fruits, more specifically in their achenes, pips, or stones [49]. The spectrum is designated as a "cellulose-like" EPR signal and consists of an intense singlet line and two weak satellite lines situated at about 30 G left and right of it. The triplet is characterized by a *g*-value that varies in the range of 2.0032 to 2.0044. The spacing with the weak satellite lines varies from 30 to 34 G depending on the origin of the cellulose. The radical associated with the triplet structure probably results from the dehydrogenation of cellulose main chains [58,59]. Based on the previous observations on irradiated fruits mentioned above and the likely radicals that can form in pitaya fruit, center III is tentatively assigned to the radical associated with the triplet spectrum (cellulose-derived radical). It was difficult to identify the triplet structure in the present study as there is an overlap from the high-intensity lines of center II radical. The center line of the triplet is quite intense and can be seen in the spectrum (Fig. 6). The satellite lines are very weak, the intensity of each one of the lines is about 3 % of the high-intensity center line [51]. Attempts based on thermal annealing experiments did not show the observance of weak lines. The results of the thermal annealing experiments are shown in Fig. 8. It is seen that the radical becomes unstable at about 50 °C and undergoes decay in the temperature range of 50 °C to 120 °C.

The time dependence of the EPR signals induced by radiation is one of the most important parameters for the correct evaluation of the amount of radiation dose to which the pitaya fruit was subjected. The stability of the free radicals induced by ionizing radiation depends on the environmental and storage conditions of the product obtained from

the fruit. The radiation energy absorbed by the sample and its stability with storage time is called fading.

To evaluate the fading of the red pitaya skin powder sample previously irradiated with a dose of 10 kGy was preserved in Pyrex tubes under normal laboratory storage conditions. Free radical fading was investigated by monitoring the change in EPR signal intensities at time intervals over a period of approximately 114 days. For a correct evaluation of the fading, we ensured that the experimental conditions and the positions of the samples in the resonant cavity of the EPR spectrometer always remained the same for each measurement.

The variation of EPR signal intensities as a function of the storage time of red pitaya skin powder irradiated with a dose of 10 kGy is shown in Fig. 10. The EPR signal intensities of the red pitaya sample decrease by about 20 % in the first 21 days, after day 30, the trend is invariant, i.e., the stability of free radicals does not depend on storage time. A similar result was observed by Paksu et al. [44] for the powdered oleaster fruits. This result shows that the EPR signal of red pitaya does not fade after prolonged storage, and demonstrates the stability of EPR signals after 30 days of storage. In addition, the stability of the EPR signals at various temperatures (Fig. 8) corroborates the fading result of red pitaya.

Once the stability studies with heat treatment and fading of EPR signals were performed, the gamma radiation dose–response of red pitaya centers II and III was investigated.

The effect of different doses of ionizing irradiation on the EPR spectra of powdered red pitaya skin was investigated by irradiating with gamma irradiation doses in the range of 500 Gy to 30 kGy. Fig. 11 shows the EPR spectra of powdered pitaya for different gamma exposure doses, presenting EPR spectra with similar formats. Furthermore, the intensity of the EPR signals due to centers II and III increase uniformly with increasing gamma dose, resulting in the generation of free radicals corresponding to centers II and III proportional to the absorbed dose.

Fig. 12 shows the behavior of the peak-peak EPR intensity of the red pitaya skin as a function of the absorbed gamma dose. In this figure, it is observed that the intensity of the EPR signals of both centers (centers II and III) increase linearly with the absorbed dose in the range of 500 Gy and 30 kGy, given that, on a logarithmic scale, the linearity is represented by the straight line with slope 1. This result and the fading result

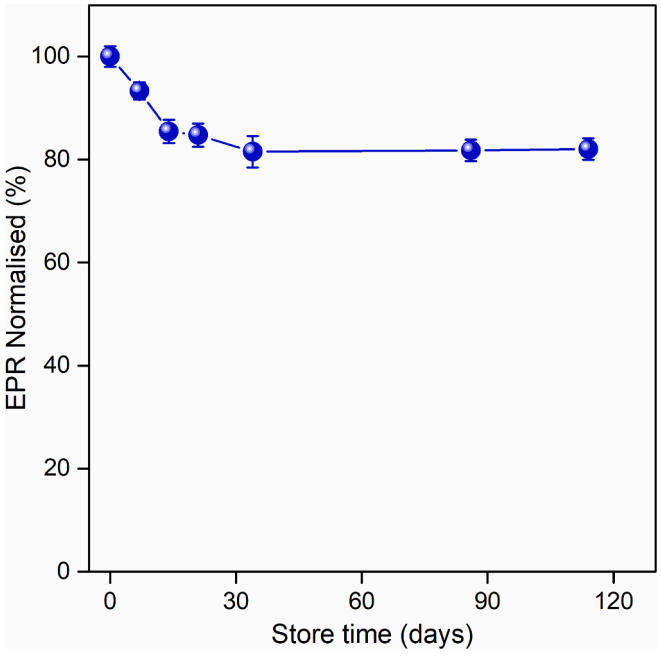

Fig. 10. EPR signal fading under the same storage conditions of red pitaya skin powder. Room temperature (23 ± 2 °C) and relative humidity (about 35 %).

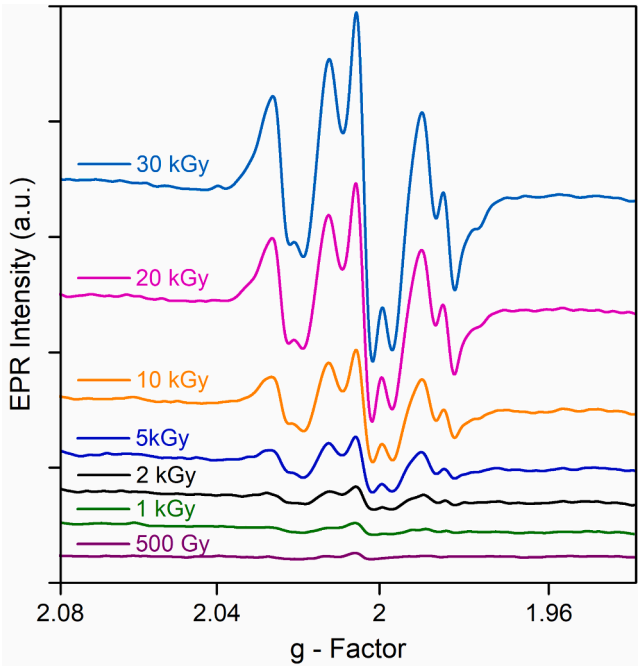

Fig. 11. EPR spectra of freeze-dried and pulverized red pitaya skin for different gamma radiation doses between 500 Gy and 30 kGy.

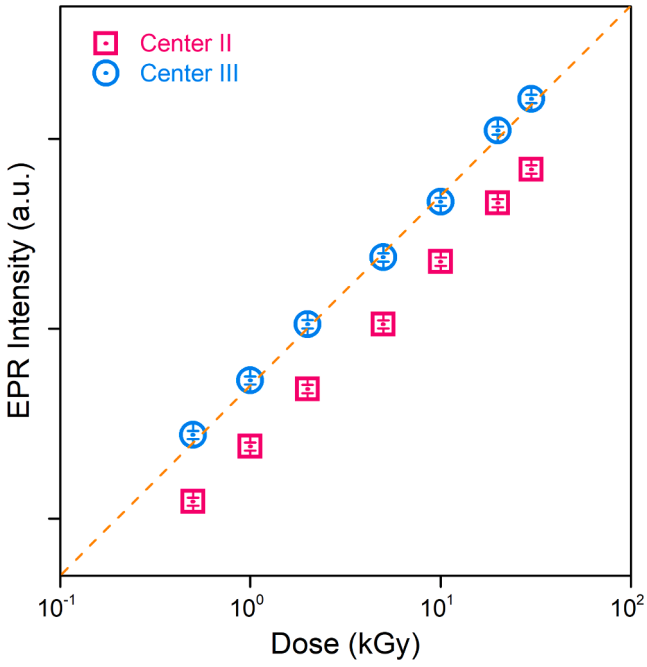

Fig. 12. Dependence of the peak-to-peak EPR intensity with an absorbed dose of centers II (red square) and center III (blue sphere) of red pitaya skin. Dashed orange line indicates linear behavior. Five replicate samples for each dose.

suggest that pitaya can be used for radiation control and dosimetry applications in the investigated dose range, that is, in the determination of the amount of dose to which the material was subjected.

4. Conclusions

SEM images evidenced the presence of pitaya grains with rough, irregular aspects and different dimensions. The structural analysis by XRD showed the presence of crystalline phases due to cellulose, glucose, and other organic and inorganic molecules, in addition to the presence

of an amorphous phase. From the XRD results, we can conclude that the crystalline and amorphous structures are unalterable with the gamma radiation dose. The presence of Mn^{2+} ion in the studied pitaya powders is detected from its EPR spectrum. Gamma irradiation induces multiple centers and their EPR signals overlap. The intensity of the six hyperfine lines of the Mn^{2+} ion remains constant with irradiation. One of the centers (center II) is due to the sugar constituent in the pitaya fruit while the cellulosic part produces center III. The lines associated with centers II and III, which are only produced by radiation, showed a linear behavior as a function of dose in the range 500 Gy and 30 kGy. The paramagnetic center associated with cellulose shows a 20 % fading in its EPR intensity during the first 21 days, remaining constant for periods longer than this time. These results suggest that the paramagnetic centers produced by radiation in pitaya skin can be used for the control and identification of irradiated products in a wide range of doses.

Declaration of competing interest

The authors declare that they have no known competing financial interests or personal relationships that could have appeared to influence the work reported in this paper.

Data availability

The data that has been used is confidential.

Acknowledgment

The authors wish to thank Ms. E. Somessari for kindly carrying out the irradiation of the pitaya samples, and the laboratory "Centro de Ciência e Tecnologia de Materiais - CCTM" for the SEM measurements, both from IPEN/CNEN-SP. In addition, the authors wish to thank Mr. Airton B.A. Silva from CEAGESP for providing the red pitaya fruits needed for the study.

References

[1] United Nations (UN), "Transforming our world: the 2030 agenda for sustainable development", Finalized text for adoption, (A/70/L.1), New York, NY, September 25, 2015.
[2] FAO, 2023 http://www.fao.org/food-loss-and-food-waste/flw-data.
[3] J. Madureira, L. Barros, S.C. Verde, F.M.A. Margaca, Ionizing radiation technologies to increase the extraction of bioactive compounds from agro-industrial residues: A review, J. Ag. Food Chem. 68 (2020) 11054–11067, https://doi.org/10.1021/acs.jafc.0c04984.
[4] S. Gupta, A.K. Nadda, A. Gupta, J. Singh, S.I. Mulla, S. Sharma, Transforming Wastes into High Value-Added Products: An Introduction, Biopolymers, Springer, 2022, pp. 1–18.
[5] M. Yusuf, Agro-Industrial Waste Materials and Their Recycled Value-Added Applications: Review. In Handbook of Ecomaterials; Martínez, L. M. T., Kharissova, O. V., Ildusovich Kharisov, B., Eds.; Springer, 2021.
[6] C.P. Feliciano, High-dose irradiated food: Current progress, applications, and prospects, Radiat. Phys. Chem. 144 (2018) 34–36, https://doi.org/10.1016/j.radphyschem.2017.11.010.
[7] I. Rossi, Q.M.A. Hasan, A review of irradiation technologies on food and agricultural products, International J. Sci. Technol. Res. 9 (2020) 4411–4414.
[8] H.M. Khan, I.A. Bhatti, H. Delincée, Thermoluminescence of contaminating minerals for the detection of radiation treatment of dried fruits, Radiat. Phys. Chem. 63 (2002) 403–406, https://doi.org/10.1016/S0969-806X(01)00630-2.
[9] G. Bayramb, H. Delincée, Identification of irradiated Turkish foodstuffs combining various physical detection methods, Food Control 15 (2004) 81–91, https://doi.org/10.1016/S0956-7135(03)00018-5.
[10] I.S. Arvanitoyannis, A.C. Stratakos, P. Tsarouhas, Irradiation applications in vegetables and fruits: A review, Crit. Rev. Food Sci. 49 (2009) 427–462, https://doi.org/10.1080/10408390802067936.
[11] M. Ikeya, New applications of Electron Spin Resonance, Dating, Dosimetry and Microscopy, World Scientific, Singapore, 1993.
[12] M. Kuvykina, A. Pryadka, V. Tenishev, A. Gorskiy, A. Aprelev, Application of the electronic paramagnetic resonance method for detecting radiation-processed food products, J. Phys.: Conf. Ser. 2192 (2022) 012023, https://doi.org/10.1088/1742-6596/2192/1/012023.
[13] A. Mishra, A. Upadhyay, P. Jaiswal, N. Sharma, Effect of different drying method on the chemical and microstructural properties of *Loquat slices*, J. Food Process. Pres. 45 (2020) e15105.
[14] I. Dankar, A. Haddarah, F.E.L. Omar, M. Pujolà, F. Sepulcre, Characterization of food additive-potato starch complexes by FTIR and X-ray diffraction, Food Chem. 260 (2018) 7–12, https://doi.org/10.1016/j.foodchem.2018.03.138.
[15] R. Paranthaman, J.A. Moses, C. Anandharamakrishnan, Novel powder-XRD method for detection of acrylamide in processed foods, Food Res. Int. 152 (2022) 110893, https://doi.org/10.1016/j.foodres.2021.110893.
[16] Y. Wu, J. Xu, Y. He, M. Shi, X. Han, W. Li, X. Zhang, X. Wen, Metabolic profiling of pitaya (*Hylocereus polyrhizus*) during fruit development and maturation, Molecules 24 (2019) 1114, https://doi.org/10.3390/molecules24061114.
[17] H. Jiang, W. Zhang, X. Li, C. Shu, W. Jiang, J. Cao, Nutrition, phytochemical profile, bioactivities and applications in food industry of pitaya (*Hylocereus spp*.) peels: A comprehensive review, Trends Food Sci, Tech. 116 (2021) 199–217, https://doi.org/10.1016/j.tifs.2021.06.040.
[18] R.M. Zaid, P. Mishra, Z. Ab Wahid, A.M. Sakinah, *Hylocereus polyrhizus* peel's high-methoxyl pectin: A potential source of hypolipidemic agent, Int. J. Biol. Macromolecules 134 (2019) 361–367, https://doi.org/10.1016/j.ijbiomac.2019.03.143.
[19] M. Utpott, R.R. Araujo, C.G. Vargas, A.R.N. Paiva, B. Tischer, A.O. Rios, S.H. Flôres, Characterization and application of red pitaya (*Hylocereus polyrhizus*) peel powder as a fat replacer in ice cream, J. Food Process. Pres. 44 (5) (2020), Article e14420. doi: 10.1111/jfpp.14420.
[20] M.H.M. Cordeiro, J.M. Silva, G.P. Mizobutsi, E.H. Mizobutsi, W.F. Mota, Physical, chemical and nutritional characterization of pink pitaya of red pulp, Rev. Bras. Frutic. 37 (2015) 20–26, https://doi.org/10.1590/0100-2945-046/14.
[21] P. Madane, A.K. Das, P.K. Nanda, S. Bandyopadhyay, P. Jagtap, A. Shewalkar, B. Maity, Dragon fruit (*Hylocereus undatus*) peel as antioxidant dietary fibre on quality and lipid oxidation of chicken nuggets, J. Food Sci. Tech. 57 (4) (2020) 1449–1461, https://doi.org/10.1007/s13197-019-04180-z.
[22] A. Montoya-Arroyo, R.M. Schweiggert, M.L. Pineda-Castro, M. Sramek, R. Kohlus, R. Carle, P. Esquivel, Characterization of cell wall polysaccharides of purple pitaya (*Hylocereus sp.*) pericarp, Food Hydrocolloid. 35 (2014) 557–564, https://doi.org/10.1016/j.foodhyd.2013.07.010.
[23] J. Taira, E. Tsuchida, M.C. Katoh, M. Uehara, T. Ogi, Antioxidant capacity of betacyanins as radical scavengers for peroxyl radical and nitric oxide, Food Chem. 166 (2015) 531–536, https://doi.org/10.1016/j.foodchem.2014.05.102.
[24] G.C. Tenore, E. Novellino, A. Basile, Nutraceutical potential and antioxidant benefits of red pitaya (*Hylocereus polyrhizus*) extracts, J. Funct. Foods 4 (2012) 129–136, https://doi.org/10.1016/j.jff.2011.09.003.
[25] Y. Zhuang, Y. Zhang, L. Sun, Characteristics of fibre-rich powder and antioxidant activity of pitaya (*Hylocereus undatus*) peels, Int. J. Food Sci. Tech. 47 (6) (2012) 1279–1285, https://doi.org/10.1111/j.1365-2621.2012.02971.x.
[26] A.R. Trindade, A. Reis, L. Sabbo, D. Trindade, P. Paiva, A. Duarte, Pitaia: perspectivas e dificuldades de uma "nova" cultura, Agrotec 30 (2019) 32–34. http://hdl.handle.net/10400.1/12431.
[27] C.T. Hsu, Y.H. Chang, S.Y. Shiau, Color, antioxidation, and texture of dough and Chinese steamed bread enriched with pitaya peel powder, Cereal Chem. 96 (2019) 76–85, https://doi.org/10.1002/cche.10097.
[28] F. Fathordoobady, A. Singh, D.D. Kitts, A.P. Singh, Hemp (Cannabis Sativa L.) extract: Anti-microbial properties, methods of extraction, and potential oral delivery, Food Ver, Int. 35 (2019) 664–684, https://doi.org/10.1080/87559129.2019.1600539.
[29] EN Protocol EN 1786, Detection of irradiated food containing bone: analysis by electron paramagnetic resonance. European Committee for Standartization, Brussels (1997).
[30] EN Protocol EN 1787, Determination of irradiated food containing cellulose: analysis by EPR. European Committe for Standartization, Brussels (2000).
[31] EN Protocol EN 13708, Detection of irradiated food containing crystalline sugar: analysis by EPR. European Committe for Standartization, Brussels (2001).
[32] M.P. Esteves, M.E. Andrade, J. Empis, Detection of prior irradiation of dried fruits by electron spin resonance (ESR), Radiat. Phys. Chem. 55 (1999) 737–742, https://doi.org/10.1016/S0969-806X(99)00304-7.
[33] M.F. Desrosiers, W.L. McLaughlin, Examination of gamma-irradiated fruits and vegetables by electron spin resonance spectroscopy, Radiat. Phys. Chem. 34 (1989) 895–898, https://doi.org/10.1016/1359-0197(89)90326-3.
[34] S.L. Chia, G.H. Chong, Effect of drum drying on physico-chemical characteristics of dragon fruit peel (*Hylocereus polyrhizus*), Int. J. Food Eng. 11 (2015) 285–293, https://doi.org/10.1515/ijfe-2014-0198.
[35] N.H. Taharuddin, R. Jumaidin, M.R. Mansor, F.A.M. Yusof, R.H. Alamjuri, Characterization of potential cellulose from *hylocereus polyrhizus* (dragon fruit) peel: a study on physicochemical and thermal properties, J. Renew. Mater. 11 (2023) 131–145, https://doi.org/10.32604/jrm.2022.021528.
[36] J.V. Kumbhar, J.M. Rajwade, K.M. Paknikar, Fruit peels support higher yield and superior quality bacterial cellulose production, Appl. Microbiol Biotechnol. 99 (2015) 6677–6691, https://doi.org/10.1007/s00253-015-6644-8.
[37] E.D. Kasapoğlu, S. Kahraman, F. Tornuk, Extraction optimization and characterization of cellulose nanocrystals from apricot pomace, Foods 12 (2023) 746, https://doi.org/10.3390/foods12040746.
[38] T. Truong, D. Dahal, P. Urrutia, L. Alvarez, S. Almonacid, B. Bhandari, Crystallisation and glass transition behaviour of Chilean raisins in relation to their sugar compositions, Food Chem. 311 (2020) 125929, https://doi.org/10.1016/j.foodchem.2019.125929.
[39] N. Harnkarnsujarit, S. Charoenrein, Effect of water activity on sugar crystallization and β-carotene stability of freeze-dried mango powder, J. Food Eng. 105 (2011) 592–598, https://doi.org/10.1016/j.jfoodeng.2011.03.026.
[40] M.C. Otálora, A. Wilches-Torres, J.A.G. Castaño, Mucilage from yellow pitahaya (*selenicereus megalanthus*) fruit peel: extraction, proximal analysis, and molecular

characterization, Molecules 28 (2023) 786, https://doi.org/10.3390/molecules28020786.
[41] P.H.F. Pereira, V. Arantes, B.H.L.O. Pereira, D.M. Oliveira, S.H. Santagneli, M.O. H. Cioffi, Effect of the chemical treatment sequence on pineapple peel fiber: chemical composition and thermal degradation behavior, Cellulose 29 (2022) (2022) 8587–8598, https://doi.org/10.1007/s10570-022-04806-0.
[42] E.F.O. Jesus, A.M. Rossi, R.T. Lopes, An ESR study on identification of gamma-irradiated kiwi, papaya and tomato using fruit pulp, International J. Food Sc. Technol. 34 (1999) 173–178, https://doi.org/10.1046/j.1365-2621.1999.00250.x.
[43] A. Chiappinelli, M. Mangiacotti, M. Tomaiuolo, G. Trotta, G. Marchesani, A. E. Chiaravalle, Identification of X-ray-irradiated hazelnuts by electron spin resonance (ESR) spectroscopy, Eur. Food Res. Technol. 245 (2019) 2323–2329, https://doi.org/10.1007/s00217-019-03349-2.
[44] U. Paksu, B. Engin, Ü. Sayın, ESR spectroscopy study of radicals induced by gamma radiation in oleaster (*Elaeagnus Angustifolia L.*) fruits, Eur. Phys. J. plus 137 (2022) 941, https://doi.org/10.1140/epjp/s13360-022-03155-y.
[45] A.M. Maghraby, E. Salama, S.A. Anwar, M. El-Sayed, Identification and dosimetry of irradiated pistachio (*Pistacia vera L.*) using EPR, Radiat. Eff. Defect. S. 178 (2023) 406–416, https://doi.org/10.1080/10420150.2022.2148251.
[46] C. Saenjum, T. Pattananandecha, K. Nakagawa, Antioxidative and anti-inflammatory phytochemicals and related stable paramagnetic species in different parts of dragon fruit, Molecules (2021) 3565. doi: 10.3390/molecules26123565.
[47] A. Abragam, B. Bleaney, Electron Paramagnetic Resonance of Transition ions, Clarendon Press, Oxford, 1970.
[48] N.D. Yordanov, K. Aleksieva, X- and Q-band EPR, studies on fine powders of irradiated plants. New approach for detection of their radiation history by using Q-band EPR spectrometry, Radiat. Phys. Chem. 69 (2004) 59–64, https://doi.org/10.1016/S0969-806X(03)00399-2.
[49] J.J. Raffi, J.P.L. Agnel, Electron spin resonance identification of irradiated fruits, Radiat. Phys. Chem. 34 (1989) 891–894, https://doi.org/10.1016/1359-0197(89)90325-1.
[50] J.J. Raffi, J.P.L. Agnel, L.A. Buscarlet, C.C. Martin, Electron spin resonance identification of irradiated strawberries, J. Chem. Soc. Faraday Trans. I (84) (1988) 3359–3362, https://doi.org/10.1039/F19888403359.
[51] N.D. Yordanov, Z. Pachova, Gamma-irradiated dry fruits: An example of a wide variety of long-time dependent EPR spectra, Spectrochim. Acta Part A 63 (2006) 891–895, https://doi.org/10.1016/j.saa.2005.10.023.
[52] H. Shields, P. Hamrick, X-irradiation damage of sucrose single crystal, J. Chem. Phys. 37 (1962) 202–203, https://doi.org/10.1063/1.1732964.
[53] G. Lomaglio, Résonance paramagnétique électronique et susceptibilité paramagnétique d'un monocristal de saccharose irradié, C.R, Séances Acad. Sci. Ser. B 264 (1967) 1637–1639.
[54] A. Gräslund, G. Löfroth, Free radicals in gamma-irradiated single crystals of trehalose dihydrate and sucrose studied by electron paramagnetic resonance, Acta Chem. Scand. Ser B 29 (1975) 475–482, https://doi.org/10.3891/acta.chem.scand.29b-0475.
[55] E. Sagstuen, A. Lund, O. Awadelkarim, M. Lindgren, J. Westerling, Free radicals in x-irradiated single crystals of sucrose: a reexamination, J. Phys. Chem. 90 (1986) 5584–5588, https://doi.org/10.1021/j100280a022.
[56] G. Vanhaelewyn, J. Sadlo, F. Callens, W. Mondelaers, D.D. Frenne, P. Matthys, A decomposition study of the EPR spectrum of irradiated sucrose, Appl. Radiat. Isotopes 52 (2000) 1221–1227, https://doi.org/10.1016/S0969-8043(00)00075-0.
[57] M. Kikuchi, Y. Shimoyama, M. Ukai, Y. Kobayashi, ESR detection procedure of irradiated papaya containing high water content, Radiat. Phys. Chem. 80 (2011) 664–667, https://doi.org/10.1016/j.radphyschem.2011.01.008.
[58] E.Y. Davydov, G.B. Pariiskii, D.Y. Toptygin, Izvestiya Akad. Nauk SSSR Ser. Khim. 8 (1984) 1747.
[59] H. Kubota, Y. Ogiwara, K. Matsuzaki, Photo-induced radicals in glucose and cellobiose, J. Appl. Polym. Sci. 19 (1975) 1291–1296, https://doi.org/10.1002/app.1975.070190509.